

Possibility of Chargino Search at LEP II

A.S.Belyaev^{a,1}, A.V.Gladyshev^{b,c,2}

^a *Skobeltsin Institute for Nuclear Physics, Moscow State University,
119 899, Moscow, RUSSIA*

^b *Bogoliubov Laboratory of Theoretical Physics, Joint Institute for Nuclear Research,
141 980 Dubna, Moscow Region, RUSSIA*

^c *Physics Department, Moscow State University, 119 899, Moscow, RUSSIA*

Abstract

We study the potential of the LEP200 collider for chargino production and the possibility of the determination of some fundamental SUSY parameters through the relation with this study. Total cross sections for two basic signatures of pair chargino production and for main backgrounds are calculated. The set of kinematic cuts is proposed for the effective background suppression and extraction of the signal. Calculations and the MC simulation performed give the limits on chargino and neutralino masses that could be obtained at LEP200 with $\sqrt{s} = 200$ GeV.

¹e-mail: belyaev@monet.npi.msu.su

²e-mail: gladyshev@thsun1.jinr.dubna.su

1 Introduction

Supersymmetry [1] is supposed to be the most promising key for the solution of problems of the Standard Model. That is why in recent years the search for SUSY has become one of the most important tasks for the present and future accelerators.

According to the great variety of models with different assumptions there are several particles which could have a mass within the reach of present or forthcoming experiments. Among these particles are: the lightest Higgs boson, the lightest neutralino, and the lightest chargino.

The Higgs boson, even if it is discovered at LEP II, will not give us complete evidence that SUSY takes place. The neutralino discovery at present is been questioned, since its production cross section is rather small and the signature is hardly separated from background events [2]. All this makes chargino the most promising superparticle to be discovered soon if *there is* supersymmetry in the nature.

In this paper we analyse a possible chargino detection via its creation in e^+e^- collisions with subsequent 'leptonic' or 'hadronic' decay. We define these decay modes as follows: the neutralino, neutrino, and the lepton or neutralino and quark pair (jets) in the final state, respectively.

To study the real possibility to detect the signal from chargino, the MC generator for the signal and background has been created. We have also included the effects of detector resolution and hadronization effects into our analysis. All squared matrix elements and the most part of numerical calculations have been made by the CompHEP package [4], in which we have implemented the part of supersymmetric standard model relevant for our analysis.

The paper is organized as follows. In Section 2, we present a brief description of the model we have used and discuss the theoretical and experimental motivations for the choice of input parameters. Then, in Section 3, we discuss possible modes of chargino decays, present the chargino production rate at LEP II and perform the MC simulation and kinematical analysis of the signal and background for different signatures with the aim to extract the signal and suppress the background. As a result of this analysis, we designed an effective set of kinematical cuts. These cuts allow one to extract the signal from the chargino up to the collider kinematic limit. In Section 4, we examine the MSSM parameters space and explore the regions which could be excluded by the analysis of chargino search at LEP II. Then we make some final conclusions.

2 The Model

2.1 Basic assumptions

The framework of the present studies is the Minimal Supersymmetric Standard Model (MSSM) [3] which has already shown itself to good advantage. It is the simplest extension of the Standard Model (SM) that makes good use of the idea of supersymmetry as an underlying principle. Supersymmetry provides solutions to some of the inner problems of SM offering a number of theoretically beautiful ways. Also, in the context of Grand Unification idea it allows for the real unification of fundamental interactions at the scale of the order 10^{16} GeV [5].

Constituents of the model are the quarks and leptons of three generations, gauge bosons and Higgs scalar fields. To these must be added the *superpartners*, the particles that differ in spin by half a unit. Thus, every gauge field of SM has its fermionic superpartner, and every matter field has a scalar partner. Contrary to SM, one needs an additional doublet of Higgs scalar fields to give masses to up quarks and to down quarks and leptons and to avoid the gauge anomaly.

An appropriate mathematical language to describe a supersymmetric model is the language of superfields. The Yukawa interactions are defined by the superpotential that in the case of MSSM reads

$$W = \epsilon_{ij} \left(h_E L^j E^c H_1^i + h_D Q^j D^c H_1^i + h_U Q^j U^c H_2^i + \mu H_1^i H_2^j \right) \quad (1)$$

Here Q and L are the left-handed quarks and leptons superfield doublets; U^c, D^c, E^c , superfields corresponding to the right-handed quarks and leptons; and $H_{1,2}$ are the Higgs superfields; i and j are the $SU(2)$ indices ($\epsilon_{12} = 1$), color and flavor indices being understood.

Since we do not observe the exact supersymmetry in the nature, *i.e.* there are no pairs of particles we could identify as superpartners, it is a broken symmetry. At present *there is* a phenomenologically acceptable way to break supersymmetry, to include the soft breaking terms into the SUSY lagrangian. *Soft*, in this context, means that these terms do not introduce new quadratic divergences into the theory. It is assumed that breaking of supersymmetry takes place in the hidden sector which interacts with the visible world only via gravity. All the possible soft terms have been studied in Ref. [6]. The SUSY breaking terms in MSSM are the mass terms for the scalars, the mass terms for the gauginos and Yukawa type terms:

$$\begin{aligned} -L_{SB} = & m_0^2 \sum_i |\phi_i|^2 + \left(\frac{1}{2} m_{1/2} \sum_\alpha \lambda_\alpha \lambda_\alpha \right. \\ & \left. + A \left(h_E l^j e^c h_1^i + h_D q^j d^c h_1^i + h_U q^j u^c h_2^i \right) + B\mu h_1^i h_2^j + h.c. \right) \end{aligned} \quad (2)$$

In general, MSSM contains too many new unknown parameters and. To reduce the number of them, one usually makes a number of simplifying assumptions. Some of them come from the Grand Unified Theories and/or Supergravity theories. The most often used are the gauge couplings unification and the universality of the soft supersymmetry breaking terms at the GUT scale, and radiative breaking of the $SU(2) \times U(1)$ symmetry at the electroweak scale. We assume also the R -parity conservation, which means, in particular, that superparticles can be produced only in pairs, and there exists the *stable* lightest supersymmetric particle (LSP) which is usually considered the lightest neutralino.

After the above-mentioned assumptions are made only five new parameters are left:

$$m_0, m_{1/2}, \mu, A, \tan \beta,$$

where m_0 is a common mass for scalars at the unification scale, $m_{1/2}$ is the same for fermions, μ is the Higgs mixing parameter, A is the soft supersymmetry breaking parameter and $\tan \beta$ is the ratio of vacuum expectation values of the two Higgs fields $\tan \beta = v_2/v_1$.

Fermionic partners of the electroweak gauge and Higgs bosons (gauginos and higgsinos) mix to give the mass eigenstates called the chargino and neutralino.

Masses can be obtained by the diagonalization of the mass matrices:

$$M^{(c)} = \begin{pmatrix} M_2 & \sqrt{2}M_W \sin \beta \\ \sqrt{2}M_W \cos \beta & \mu \end{pmatrix} \quad (3)$$

$$M^{(0)} = \begin{pmatrix} M_1 & 0 & -M_Z \cos \beta \sin \theta_W & M_Z \sin \beta \sin \theta_W \\ 0 & M_2 & M_Z \cos \beta \cos \theta_W & -M_Z \sin \beta \cos \theta_W \\ -M_Z \cos \beta \sin \theta_W & M_Z \cos \beta \cos \theta_W & 0 & -\mu \\ M_Z \sin \beta \sin \theta_W & -M_Z \sin \beta \cos \theta_W & -\mu & 0 \end{pmatrix} \quad (4)$$

M_2 is the mass of the wino, whereas M_1 is the mass of the $U(1)_Y$ gaugino, the bino. The eigenvalues corresponding to the chargino masses are

$$\tilde{m}_{\chi_{1,2}^\pm}^2 = \frac{1}{2} \left[M_2^2 + \mu^2 + 2M_W^2 \pm \sqrt{(M_2^2 - \mu^2)^2 + 4M_W^4 \cos^2 2\beta + 4M_W^2(M_2^2 + \mu^2 + 2M_2\mu \sin 2\beta)} \right].$$

The neutralino masses \tilde{m}_{χ^0} are roots λ_k of the quartic equation $F(\lambda) = 0$, where

$$\begin{aligned} F(\lambda) &= \lambda^4 - (M_1 + M_2)\lambda^3 - (M_Z^2 + \mu^2 - M_1M_2)\lambda^2 \\ &+ [(M_2 \sin^2 \theta_W + M_1 \cos^2 \theta_W - \mu \sin 2\beta)M_Z^2 + (M_1 + M_2)\mu^2]\lambda \\ &+ [(M_2 \sin^2 \theta_W + M_1 \cos^2 \theta_W)\mu M_Z^2 \sin 2\beta - M_1M_2\mu^2] \end{aligned} \quad (5)$$

The diagonalization can be performed in a straightforward way by multiplying the mass matrices by unitary rotating matrices:

$$U^T M^{(c)} V = M_{diag}^{(c)}, \quad N^T M^{(0)} N = M_{diag}^{(0)} \quad (6)$$

$$U = O_-, \quad V = \begin{cases} O_+, & \det M^{(c)} \geq 0 \\ \sigma_3 O_+, & \det M^{(c)} < 0 \end{cases}, \quad O_\pm = \begin{pmatrix} \cos \phi_\pm & \sin \phi_\pm \\ -\sin \phi_\pm & \cos \phi_\pm \end{pmatrix}, \quad (7)$$

and the angles ϕ_\pm are defined by

$$\tan 2\phi_- = 2\sqrt{2} \frac{\mu \sin \beta + M_2 \cos \beta}{M_2^2 - \mu^2 - 2M_W^2 \cos 2\beta} \quad (8)$$

$$\tan 2\phi_+ = 2\sqrt{2} \frac{\mu \cos \beta + M_2 \sin \beta}{M_2^2 - \mu^2 - 2M_W^2 \cos 2\beta} \quad (9)$$

The diagonalizing matrices U , V , and N enter into the Feynman rules.

2.2 Model parameters

In this subsection we describe the constraints imposed on the model parameters and the experimental limits on masses of SUSY particles³.

³The supersymmetric Standard Model with parameters restricted by experimental constraints is often referred to as the Constrained Minimal Supersymmetric Standard Model.

Since we are dealing with the chargino and neutralino, not all the parameters mentioned in the above discussion are relevant for our study. As has been mentioned in *e.g.* [7], the physical properties of the chargino and neutralino depend on μ , $m_{1/2}$ and $\tan\beta$, which can be easily seen from the mass matrices.

Numerical values of the parameters should obey some common restrictions. For example, if one wants supersymmetry to solve the hierarchy problem, the masses of superpartners have to be below 1 TeV. This leads to some obvious boundaries in the parameter space. Usually it is supposed that

$$\begin{aligned}
-1000 \text{ GeV} &\lesssim \mu \lesssim 1000 \text{ GeV}, \\
0 &\lesssim m_{1/2} \lesssim 1000 \text{ GeV}, \quad 1 \leq \tan\beta \leq 50
\end{aligned}
\tag{10}$$

Among the experimental constraints that can be imposed on the model parameters the *top-mass constraint* deserves special comment. It has been shown in Ref. [8] that once it is taken into account ($m_t = 175 \pm 6$ GeV) one has to distinguish between two possible scenarios determined by the value of $\tan\beta$. The two allowed regions are $1 < \tan\beta < 3$ and $20 < \tan\beta < 40$. The sign of the Higgs mixing parameter μ is undetermined since the *electroweak symmetry breaking constraint* determines only μ^2 . One should note also that if the *relic density constraint* is included, only the high $\tan\beta$ scenario permits the light chargino and neutralino, which is considered the best candidate for the dark matter of the Universe. In our study we used, as input parameters, the results of the global fit analysis [8, 9]; the latter constraint has not been considered in Ref.[8], thus giving the possibility for the light chargino and neutralino for the low $\tan\beta$ scenario. From now on we shall deal with both scenarios, keeping in mind that they imply *different* sets of the basic parameters with the allowed lower mass of the chargino.

Numerical values of the parameters are presented in table 1 for scenarios with low and high $\tan\beta$. To calculate the mass spectrum of superparticles we run one-loop renormalization group equations from the unification point down to the low energy (≈ 1 TeV) region. The mass spectrum obtained is shown in table 2 for both scenarios.

3 Chargino production and decay

All analytic and numerical calculations of a $2 \rightarrow 2$ process of pair chargino production ($e^+e^- \rightarrow \chi^+\chi^-$), $2 \rightarrow 3$ processes of chargino decay, and $2 \rightarrow 4$ background processes have been done with the aid of the CompHEP software package [4]. This package allows one to perform complete tree level calculations in the framework of any fed model. For calculations in the framework of MSSM the necessary part of the model related to the process under study has been implemented into CompHEP. We used the Feynman rules written down in Ref. [10]. The model was extensively tested. One of the tests was calculations both in the *t*'Hooft-Feynman and unitarity gauges which had an agreement at the level of numerical accuracy.

The chargino is produced via *s*-channel (with γ and *Z*-boson exchange) as well as via the *t*-channel diagram with the sneutrino illustrated in fig. 1. *s*-channel and *t*-channel diagrams interfere destructively, so that the cross section has a minimum at a value of the sneutrino mass around m_{χ^+} , see fig. 2.

For the mass spectrum under study the sneutrino mass is much higher than that of the chargino and thus the t -channel diagram has a several per cent negative contribution. It is clearly illustrated in fig. 2, where the dependence of the total cross section of pair chargino production is shown as a function of the sneutrino mass for low $\tan\beta$ (solid line) and high $\tan\beta$ (dashed line) scenarios. For example, for a given sneutrino mass (407 GeV and 801 GeV) and 95 GeV chargino, cross sections are: 2.9 pb and 3.2 pb respectively, while contribution only from the s -channel diagram is 3.5 pb and 3.4 pb for these two scenarios.

For the low $\tan\beta$ scenario with a lower sneutrino mass, the negative interference is bigger than that for the high $\tan\beta$ scenario (20% in comparison with 6%). In the range of chargino mass 60-100 GeV the cross section is of order of several pb varying from 6.2 pb to 1.3 pb and from 6.7 pb to 1.5 pb for the low and high $\tan\beta$, respectively. The total cross section versus chargino mass is presented in fig. 3 for both these cases.

Since the sum of neutralino and W -boson masses is higher than the chargino mass, there is only the possibility of three-body decay for the chargino. The chargino decays into $jj + \chi^0$ or $l + \nu + \chi^0$. The complete gauge invariant set of Feynman diagrams is shown in fig. 4.

If the mass of the next-to-lightest neutralino χ_2^0 is lower than the chargino one, then it could open the cascade decay of χ_2^0 . But the difference between masses of χ_1^0 and χ_2^0 of several dozen GeV (for example, 30 GeV for the high $\tan\beta$ scenario) results in that the branching ratio of chargino decay into $\chi_1^0 + f + f'$ is about 50 times as high as that of decay $\chi_2^0 + f + f'$ into (for example, 40 times for $\chi_2^0 + f + f'$ for the 95 GeV chargino, $m_{\chi_1^0} = 40$ GeV and $m_{\chi_2^0} = 70$ GeV). In the the following we do not take the latter decay channel into account.

The main contribution to the total decay width comes from the diagram with the virtual W -boson, while the contribution from diagrams with a heavy (300-400 GeV) selectron, sneutrino and charged Higgs is fairly small (1-2%). In Table 3 we present the decay widths for the 95 GeV chargino with respective branching ratios.

Though the chargino decay width is small, it has rather short lifetime in the mass range 70-100 GeV to decay inside the detector. The decay width as a function of the chargino mass is shown in fig. 5.

As one can see, $jj + \chi^0$ or $l + \nu + \chi^0$ branching ratios are very close to jet or lepton branching ratios of the W -boson. This is due to the fact that the main contribution to decay widths comes from the diagram with the virtual W -boson decaying into two jets or the lepton and neutrino. It has been checked that these branching ratios are almost independent of the chargino mass in the interval 70-100 GeV.

The possible signatures for pair chargino production are:

- 1) two leptons (an electron or a muon) + missing P_T if two charginos decay leptonically;
- 2) a charged lepton, two jets and a missing transverse momentum in the final state if one of the charginos decays leptonically while the other has the hadronic decay mode;
- 3) four jets and a missing transverse momentum if both charginos decay hadronically.

All these signatures have the same source of background, namely, the WW one. Pure leptonic signature has the lowest rate. Moreover, two neutrinos in the final state with

large P_T cause the problem of reconstructing basic specific kinematic characteristics which are important for the signal and background separation. The last two signatures seem to be the most promising for chargino search. In this paper we have concentrated just on these two cases.

For further calculations and the MC simulation we use the chargino mass equal to 95 GeV which is almost at the limit of the maximum expected beam energy.

4 Signal and Background Study

4.1 MC simulation

To study the possibility of the signal extraction from the background, the MC generator for chargino pair production and decay has been created. It was designed as a new user process for PYTHIA 5.7/JETSET 7.4 package [11]. This generator is related with PYTHIA 5.7 by a special interface and uses FORTRAN codes for squared matrix elements produced by by CompHEP. For integration of the squared matrix element over the phase space and a consequent event simulation the Monte-Carlo generator uses the BASES/SPRING package [12]. In the same manner the generator for the real $2 \rightarrow 4$: $e^+e^- \rightarrow l + jj + \nu$ background process has also been created.

The effects of the final state radiation, hadronization and string fragmentation (by means of JETSET 7.4) have also been taken into account. For the detector simulation the LUCCELL subroutine has been used. The following resolutions which are currently available at the ALEPH detector at LEP have been used for the jet and electron energy smearing: $\sigma^{hadron}/E = 0.8/\sqrt{E}$ and $\sigma^{electron}/E = 0.19/\sqrt{E}$ [13]. In our analysis we used the cone 0.4 ($\Delta R = \sqrt{\Delta\varphi^2 + \Delta\eta^2} = 0.4$) algorithm for the jet reconstruction. The minimum E_T threshold for a cell to be considered as a jet initiator has been chosen 2 GeV while the one of summed E_T for a collection of cells to be accepted as a jet has been chosen 9 GeV.

Under the assumptions mentioned above the kinematic features of both signatures for signal and background have been studied.

4.2 $l + jj + \cancel{E}_T$ signature

Let us consider the 'mixed' mode of chargino decay with a charged lepton and two jets in the final state. The branching ratio for the chargino decay when one chargino decays into an electron or a muon; and the other one, into two jets is: $BR(\chi^{pm} \rightarrow ljj + \cancel{E}_T) = 2 \cdot (0.658 \cdot 0.228) = 0.30$. For the 95 GeV chargino the cross section of this particular channel is equal to: $\sigma(\chi^{pm} \rightarrow ljj + \cancel{E}_T) = \sigma_{tot} \cdot BR(\chi^{pm} \rightarrow ljj + \cancel{E}_T) \cdot 2.9 \cdot 0.3 = 0.9$ pb.

The main background with the same signature is the $e^+e^- \rightarrow W^+W^-$ process if one of the W 's decays leptonically and the other one decays hadronically. The total cross section of this process at the tree level for $\sqrt{s} = 200$ GeV is $\sigma = 20.24$ pb with the branching ratio of the W -bosons decay $BR(W^{pm} \rightarrow ljj + \cancel{E}_T) = 2 \cdot (0.667 \cdot 0.222) = 0.29$.

We have checked that the real $2 \rightarrow 4$ $e^+e^- \rightarrow l + jj + \nu$ process gives additional 13% to the contribution from $e^+e^- \rightarrow W^+W^-$, because of other additional diagrams. In fig. 6 we present, as an example, the complete set of Feynman diagrams for $e^+e^- \rightarrow e + \nu + u + \bar{d}$ process. Its cross section is equal to 0.78 pb, while the contribution from $e^+e^- \rightarrow W^+W^-$ is equal to 0.69 pb. It has been checked that the real $2 \rightarrow 4$ $e^+e^- \rightarrow l + jj + \nu$

process has a negligible difference in the shape distribution of main kinematic variables in comparison with $e^+e^- \rightarrow W^+W^-$ (in P_T of jets, missing P_T , the invariant di-jet and the electron-neutrino mass). Thus one can use the resonance $e^+e^- \rightarrow W^+W^-$ process with applied factor 1.13.

The total cross section of the WW background for this signature is expected to be equal to $20.24 \cdot 0.29 \cdot 1.13 = 6.6$ pb.

If we take into account the integral luminosity as high as 1000 pb^{-1} , then in terms of the number of events one can expect 900 and 6600 events, respectively, for these particular signatures.

Among the kinematic variables for separation of the signal and background which have been studied in several papers (see, *e.g.* [2, 15]) the most attractive are:

- 1) The squared missing mass defined as missing 4-momentum squared. 4-momenta can be resolved for e^+e^- because we know exactly the energies of colliding beams and momenta of outgoing detectable particles. For the background the squared missing mass has a peak around zero while for the signal with undetectable heavy neutralinos it has a peak at a value larger than $2m_{\chi^0}^2$. This fact is clearly demonstrated in fig. 7. This figure clarifies also the importance of hadronization and fragmentation effects which should be taken into account as well as the smoothing of jet and electron energies. All these effects lead to the smoothing of the missing mass distribution for the background around zero which is exactly zero at the parton level.
- 2) The invariant di-jet mass which for the WW background is concentrated around the W mass, while for the signal it has a peak around $m_{\chi^+} - m_{\chi^0}$, see fig. 9. As we can see, because of the jet reconstruction effects and energy smearing, the di-jet mass distribution for the background is shifted by approximately 10 GeV from the Z -peak to a lower value
- 3) The invariant electron-neutrino mass, which for the WW background is concentrated around the W mass, but has a peak at values higher than the W -mass because of the errors in identification of the neutrino momentum. The signal distribution for the electron-”neutrino” mass has a peak, of course, at much higher values (at 155 GeV for the 95 GeV chargino and 40 GeV neutralino).
- 4) H_T variable defined as a scalar sum of the transverse energies of the two final state quarks and E_T of the charged lepton:

$$H_T = |E_T(\text{jet1})| + |E_T(\text{jet2})| + |E_T(\text{lepton})|. \quad (11)$$

This variable which was not considered in the previous studies of SUSY particle searches at LEP, but was successfully applied to the top-quark discovery at the Tevatron [14]. It can be considered as a measure of massiveness of the final state particle. In our case H_T is softer for the signal than for the WW background because of a large mass which is gone away with two massive neutralinos. It is also a strong discriminant between the signal and background, see fig. 10.

By taking into account the specific features of the kinematic variables for the signal and background shown above, the following set of kinematic cuts has been worked out:

- 1) several general cuts: $E_{T_{lepton}} > 10$ GeV, $E_{T_{j1,2}} > 10$ GeV, isolation of the electron in terms of $\Delta R = \sqrt{\Delta\phi_{e_j}^2 + \Delta\eta_{e_j}^2} > 0.3$.
- 2) missing transverse momentum > 10 GeV, only a low cut, because the \cancel{E}_T distributions for the signal and background are similar, see fig. 11.
- 3) squared missing mass > 10000 GeV²
- 4) invariant electron-neutrino mass > 140 GeV
- 5) di-jet mass < 60 GeV
- 6) $H_T < 70$ GeV

The consecutive action of these cuts is shown in Table 4 for the number of events corresponding to the total integrated luminosity 1000 pb^{-1} . It is clearly seen that designed cuts shown above suppress the background quite enough for the signal to be subtracted. It should be pointed out that the upper edge of the di-jet mass distribution for the signal gives an important information about the chargino and neutralino mass, it is equal to $(m_{\tilde{\chi}^+} - m_{\tilde{\chi}^0})$, so the cut on the di-jet mass has been chosen in a way it does not affect the signal at all. After all cuts have been applied, we have 228 events for the signal and 15 events from the background which is reduced by factor 0.002 from the parton level.

In fig.12 the di-jet mass distribution illustrating the clear signal effect is shown after the whole set of cuts has been applied.

4.3 4 jets + \cancel{E}_T signature

Let us turn now to the signature when both charginos decay hadronically having the 4 jets + \cancel{E}_T signature. For this case the signal ratio with $BR = (0.67 \cdot 0.67) = 0.45$ is 1.5 times higher than for the first signature. So the cross section for this channel is $2.9 \cdot 0.45 = 1.3$ pb.

The main SM backgrounds leading to the 4jets + \cancel{E}_T signature are, first of all, the WW process when one W decays hadronically and the other decays into τ -neutrino and τ -lepton which decays then hadronically giving an extra neutrino and two jets. The branching ratio of this decay is $2 \cdot 1/9 [BR(W \rightarrow \tau\nu_\tau)] \cdot 2/3 [BR(W \rightarrow 2jets)] \cdot 0.65 [BR(\tau \rightarrow \nu_\tau + hadrons)] = 0.096$. Thus the cross section of this process is $22.9 \cdot 0.096 = 2.2$ pb.

We have also checked the other possible sources of backgrounds: $e^+e^- \rightarrow \nu\bar{\nu}q\bar{q}$ with the consequent gluon radiation of quarks, (for example, the cross section of the $e^- \rightarrow \nu_e\bar{\nu}_e u\bar{u}$ process is equal to 0.038 pb, and after the di-jet radiation one can expect an additional factor of α_s^2 , and the total cross section of the processes $e^+e^- \rightarrow \nu\bar{\nu}q\bar{q} \rightarrow \cancel{E}_T + 4jets$ is of order 0.001 pb); $e^+e^- \rightarrow \nu_e\bar{\nu}_e W^+W^-$ process with the total cross section $7.5 \cdot 10^{-7}$ pb and $e^+e^- \rightarrow \nu_e\bar{\nu}_e Z^0Z^0$ process with the total cross section $5.4 \cdot 10^{-9}$ pb. We can see that the only real background is the first one mentioned above.

For the 1000 pb^{-1} luminosity we can expect 1300 and 2200 events of the signal and background, respectively, with the ratio higher than for the previous signature. At the same time MC simulation shows that it is more difficult to extract the signal for that type of events. The missing mass distribution for the signal is softer than that for the $lepton + 2jets + \cancel{E}_T$ signature because of the absence of the neutrino, while for the background it is wider and harder because of the presence of additional neutrinos after the τ -lepton

decay. Also, for the $4jet + \cancel{E}_T$ signature there is no lepton in the final state and we cannot use the invariant mass of a lepton and a neutrino as a discriminator of the background.

There is the reason for the fact that the signal ratio for $4jet + \cancel{E}_T$ becomes smaller than for $lepton + 2jets + \cancel{E}_T$ signature after the detector simulation. It is related to the probability of the jet to be reconstructed. For WW events this probability is higher than that for chargino production with softer jets coming from virtual W -boson with effective mass of 40 GeV which is half as large as that for the real W -boson. The estimated probability (for parameters under the assumption) of the jet reconstruction from the real W -boson is about 90% while for the virtual W -boson it is only 70%. It means that the signal with two or four jets loses 50% or 75% events respectively. This fact makes also the $lepton + 2jets + \cancel{E}_T$ signature a little bit more attractive for the chargino search.

At the same time the $4 - jet + \cancel{E}_T$ channel is complementary to the $l + 2jet + \cancel{E}_T$ one and can give information about the branching ratios of chargino decay; it would be an independent confirmation of the possible chargino existence.

For the background reduction we chose kinematical variables similar to those for the previous signature:

- 1) Squared missing mass. For the background it has a peak around zero, but this distribution, as it was told above, is wider than that for the $l + 2jet + \cancel{E}_T$ events and softer for the signal, see fig. 13.
- 2) Invariant four-jet mass, which for the WW -background is concentrated around $2M_W$, while for the signal it has a peak around $2m_{\chi^+} - m_{\chi^0}$, see fig. 14.
- 3) H_T variable, see fig. 15.

The following set of kinematic cuts has been designed for this signature:

- 1) several general cuts: $E_{Tj1,2,3,4} > 10$ GeV,
- 2) missing transverse momenta > 15 GeV, to reject a big amount of events which have nothing to do with the τ -lepton in the final state. Usually these events are from the 4-jet WW -decay with small missing transverse momenta, see fig. 16.
- 3) squared missing mass > 5000 GeV²
- 4) four-jet mass < 120 GeV
- 5) $H_T < 100$ GeV

The consecutive action of these cuts is shown in Table 5 for the number of events corresponding to the same integrated luminosity as before. It is also clearly seen that the designed cuts suppress the background quite enough for the signal to be subtracted.

After all cuts have been applied, we have 261 events for the signal and 43 from the background which is reduced by factor 0.02. We can see that the reduction factor for the background for this signature is 10 times smaller than that for the $l + 2jets + \cancel{E}_T$ signature for the reasons explained above. But nevertheless the cuts for the "jet" signature have a big affect on the background. In fig.17 the four-jet mass distribution, with clear signal effect similar to the previous signature, is shown after the whole set of cuts has been applied.

The upper edges of the four-jet mass distribution determine the $2 \cdot (m_\chi^+ - m_\chi^0)$ value which should be consistent with the value $(m_\chi^+ - m_\chi^0)$ coming from the $l + 2jets + \cancel{E}_T$ signature study and it is complementary, which can improve determination of the chargino and neutralino masses. The procedure of extracting information about the chargino and neutralino from the endpoints of M_{jj} and E_{jj} has been described in [15]. The same procedure should be used in the case of the endpoints for M_{jjjj} and E_{jjjj} . The accuracy of the determination of the chargino and neutralino mass is expected to be of order 5 GeV.

5 Conclusions

In this paper, we have investigated the potential of the LEP II collider for the search of the chargino signal. The charged fermion, light chargino, is the most preferable SUSY particle to be discovered the first at LEP II.

The total production rate of pair chargino production has been calculated. In the mass range within the reach of LEP II, the cross section of chargino production is of order 1 pb.

The decay channels of the chargino have been studied. The only possibility of three-body decay is shown. The decay width as well as branching ratios have been calculated. It is shown that decay of the chargino into the next-to-lightest neutralino (which opens the cascade decay of the chargino) is suppressed enough for not to be taken into account. The most preferable signatures for chargino search, namely $lepton + 2jets + \cancel{E}_T$ and $4jets + \cancel{E}_T$ have been studied. The signature with four jets and missing transverse momenta has not been investigated in details before.

For analysing of the signal and background kinematics in order to suppress the latter, the MC generator has been created. In comparison with the previous papers related to the chargino search at LEP II, not only smearing but also the effects of hadronization and jet reconstruction as well as final state radiation have been taken into account, which is especially important for the $4 - jets + \cancel{E}_T$ signature. Based on the study of the signal and background kinematics, the set of cuts for the signal extraction has been designed. These cuts suppress the background quite enough for the signal to be clearly seen. The information about chargino and neutralino masses can be extracted from the endpoints of the M_{jj} and E_{jj} or M_{jjjj} and E_{jjjj} distributions with an accuracy of order 5 GeV.

The limits on the chargino mass which could be obtained at LEP II is very close (1-2 GeV) to the kinematic limit of the machine. The chargino discovery would shed light on the supersymmetry parameter space especially on $m_{1/2}$ and μ which are directly related to the chargino and neutralino masses. One can draw the chargino mass as a 2-D function of the $m_{1/2}$ and μ parameters (fig. 18 for low $\tan\beta$ and fig. 20 for high $\tan\beta$ scenarios) and study the limits of $m_{1/2}$ and μ for a fixed chargino mass which will be obtained at LEP II. In fig. 19 (low $\tan\beta$) and fig. 21 (high $\tan\beta$) two regions in the $m_{1/2}$ and μ plane are shown excluding SUSY parameters for the 85 GeV (the present limit) and 99 GeV (the limit for $\sqrt{s} = 200$ GeV) chargino. For example, for typical values of $\mu = 500$ and 1000 GeV the limit on $m_{1/2}$ can be extended for the low $\tan\beta$ scenario from 75 up to 100 GeV and from 80 to 107 GeV, respectively, for LEP II with $\sqrt{s} = 200$ GeV. For high $\tan\beta$ the respective limits will be extended from 101 to 118 GeV for $\mu = 500$ GeV and from 102 to 121 GeV for $\mu = 100$ GeV.

Acknowledgments

We would like to thank D.I. Kazakov and W. de Boer for valuable discussions and comments. We are also grateful to all members of the CompHEP group for the help in adapting CompHEP for the SUSY model and useful discussions, especially, to E.Boos, V.Ilyin and A.Pukhov.

The financial support of the Russian Foundation for Basic Research (grants # 96-02-17379-a, #96-02-19773-a) and ICFPM in 1996 is acknowledged.

References

- [1] Y.Gol'fand and E.Likhtman, JETP Lett. **13** (1971) 323,
D.Volkov and V.Akulov, Phys.Lett. **B46** (1973) 109,
J.Wess and B.Zumino, Nucl.Phys. **B70** (1974) 39;
- [2] J.-F.Grivaz, Proceedings of the Workshop "Properties of Supersymmetric Particles, Erice, Italy, 1992;
- [3] For review and original references see
N.P.Nilles, Phys.Rep. **110** (1984) 1,
H.E.Haber, G.L.Kane, Phys.Rep. **117** (1985) 75,
R.Barbieri, Riv.Nuovo Cim. **11** (1988) 1;
- [4] E.E.Boos et al., hep-ph/9503280,SNUTP-94-116;
E.E.Boos et al., in Proc. of the Xth Int. Workshop on High Energy Physics and Quantum Field Theory, QFTHEP-95, ed. by B.Levtchenko, and V.Savrin, (Moscow, 1995), p.101
- [5] U.Amaldi, W. de Boer, H.Fürstenau, Phys.Lett., **B260** (1991) 447;
- [6] L.Girardello, M.T.Grisaru, Nucl.Phys. **B194** (1982) 65.
- [7] J.F.Gunion, H.E.Haber, Nucl.Phys. **B272** (1986) 1, **B402** (1993) 567;
- [8] W. de Boer, R.Ehret, D.I.Kazakov, Z.Phys. **C67** (1995) 647;
- [9] W. de Boer et al., Z.Phys. **C71** (1996) 415;
- [10] J.Rosiek, Phys.Rev.D41, 3464 (1990)
- [11] T. Sjöstrand, Comp.Phys.Comm. **82** (1994) 74;
- [12] S.Kawabata, Comp.Phys.Comm. **41** (1996) 127;
- [13] ALEPH Collaboration (D.Decamp et al.), Phys.Rep. **216** (1992) 253;
- [14] D0 collaboration (S.Abachi et al.) Phys.Rev.Lett. **74** (1995) 2632;
- [15] J.L.Feng, M.J.Strassler, Phys.Rev. **D51** (1995) 4661;

Figures

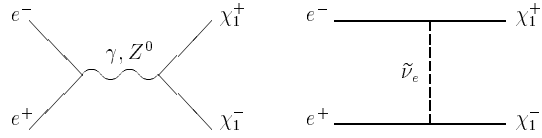


Figure 1: Diagrams for the pair chargino production in e^+e^- collisions.

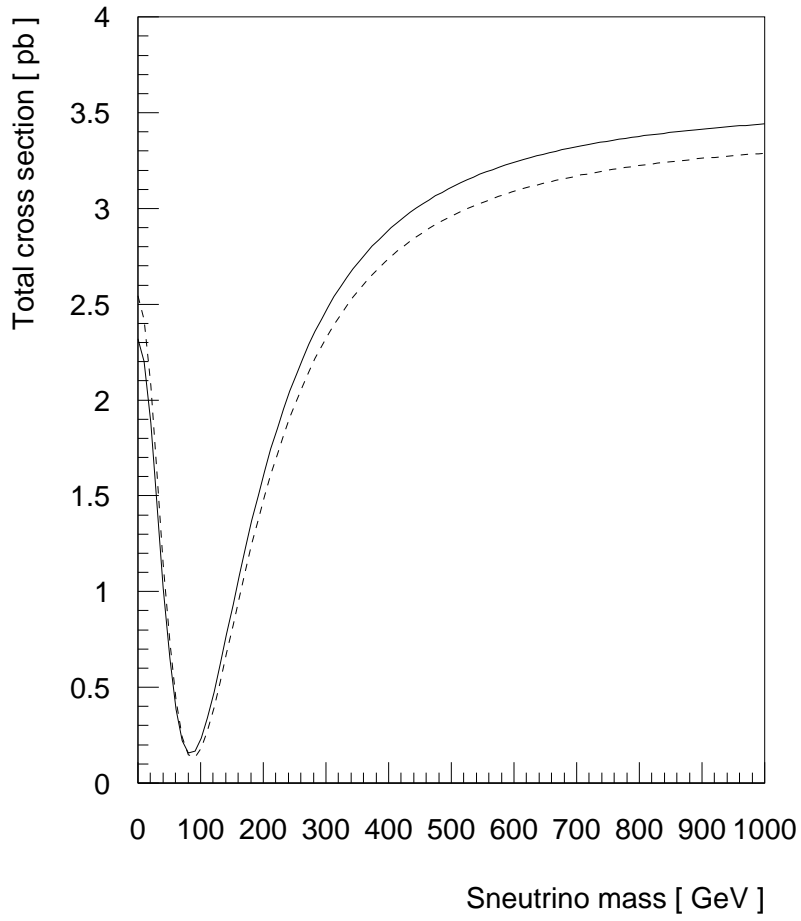


Figure 2: The cross section as a function of the sneutrino mass for the low $\tan\beta$ (solid line) and high $\tan\beta$ scenarios ($m_{\chi_{\pm}}=95$ GeV).

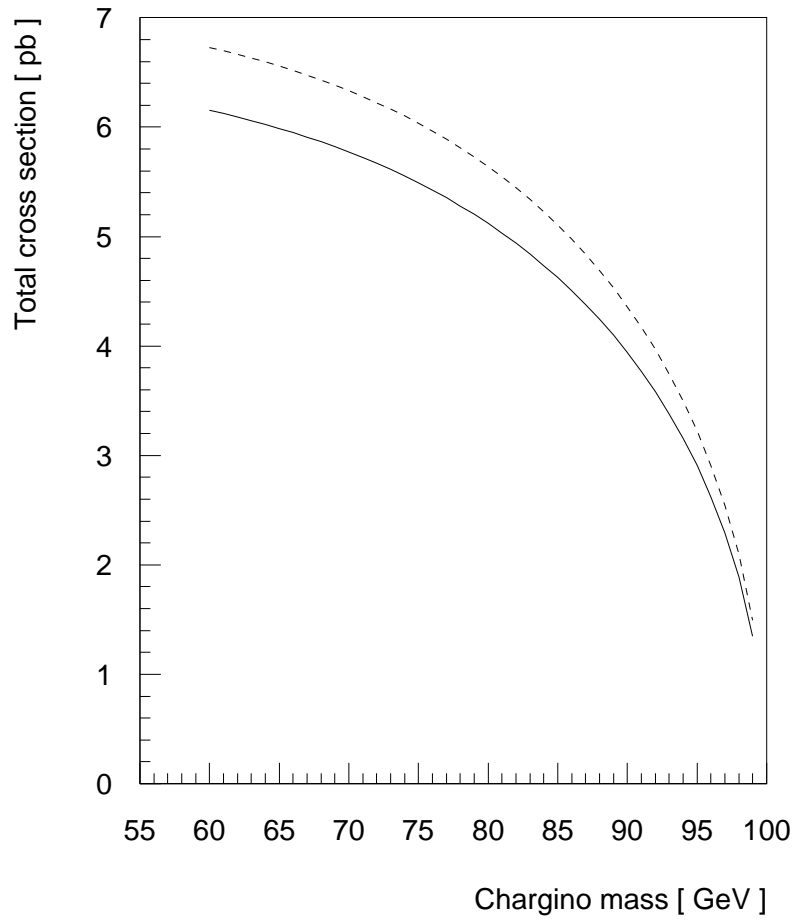


Figure 3: The cross section as a function of the chargino mass for the low $\tan\beta$ (solid line) and high $\tan\beta$ scenarios.

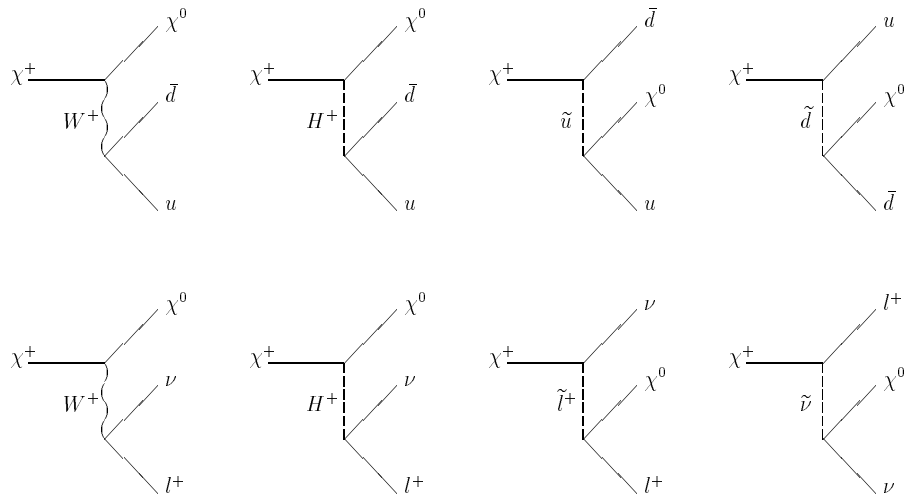


Figure 4: Diagrams for the chargino decay modes.

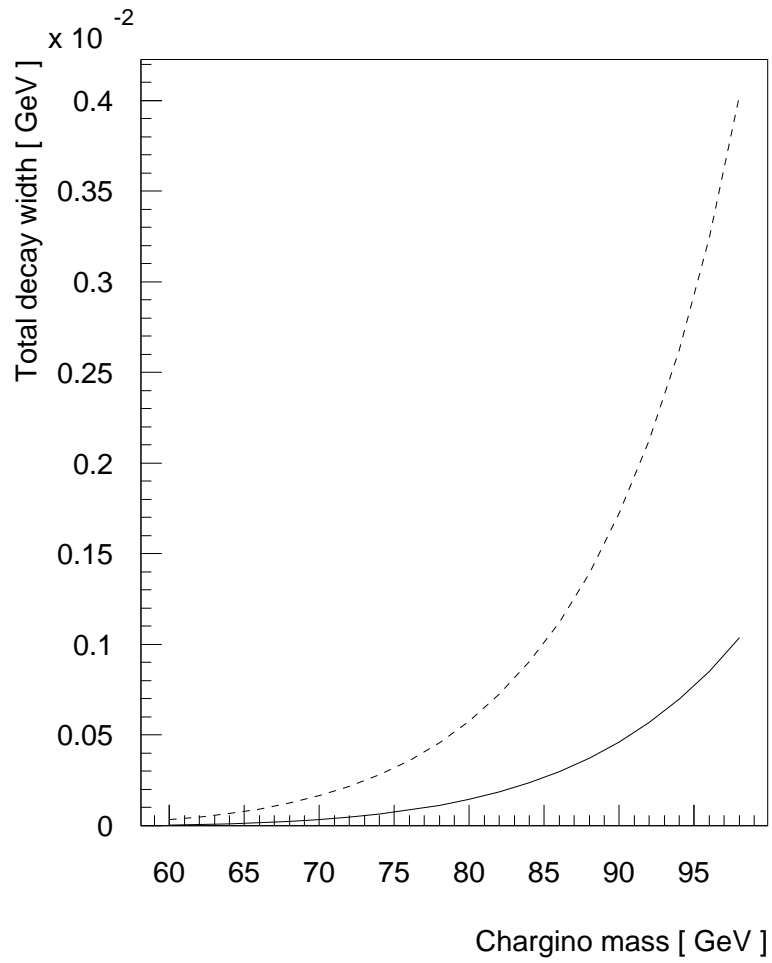


Figure 5: The total decay width as a function of the chargino mass for the low $\tan\beta$ (solid line) and high $\tan\beta$ scenarios.

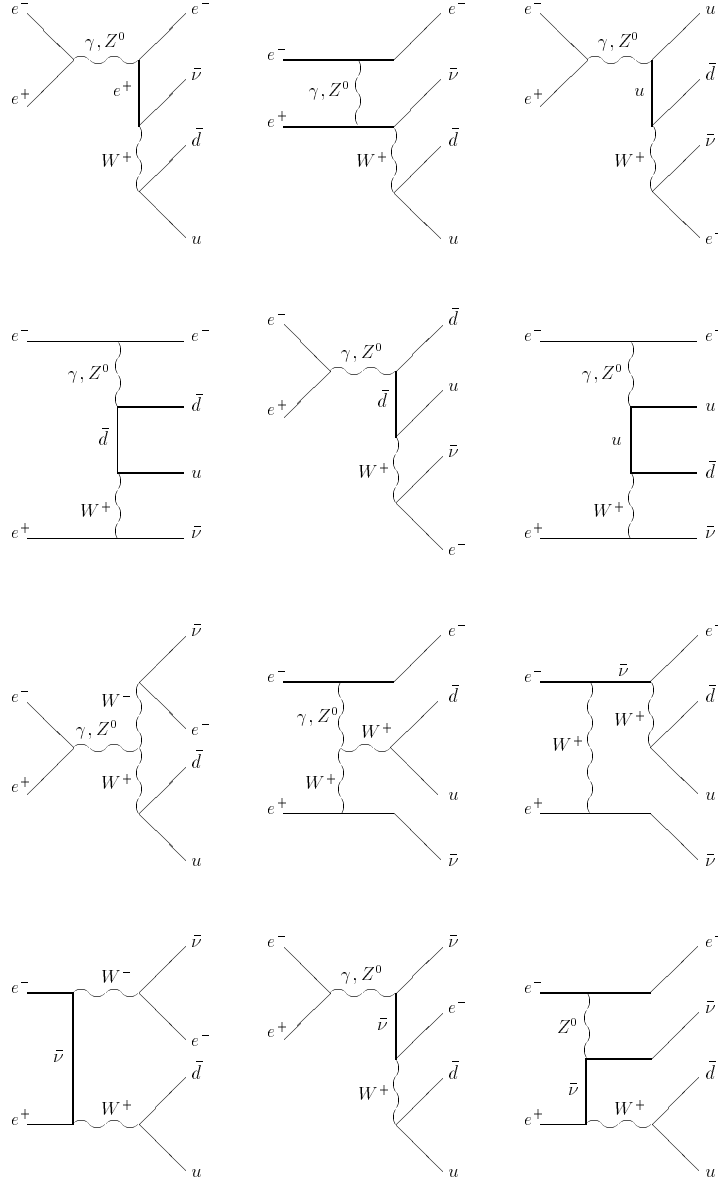


Figure 6: The complete set of diagrams for the $e^+e^- \rightarrow e^-\bar{\nu}d\bar{u}$ process

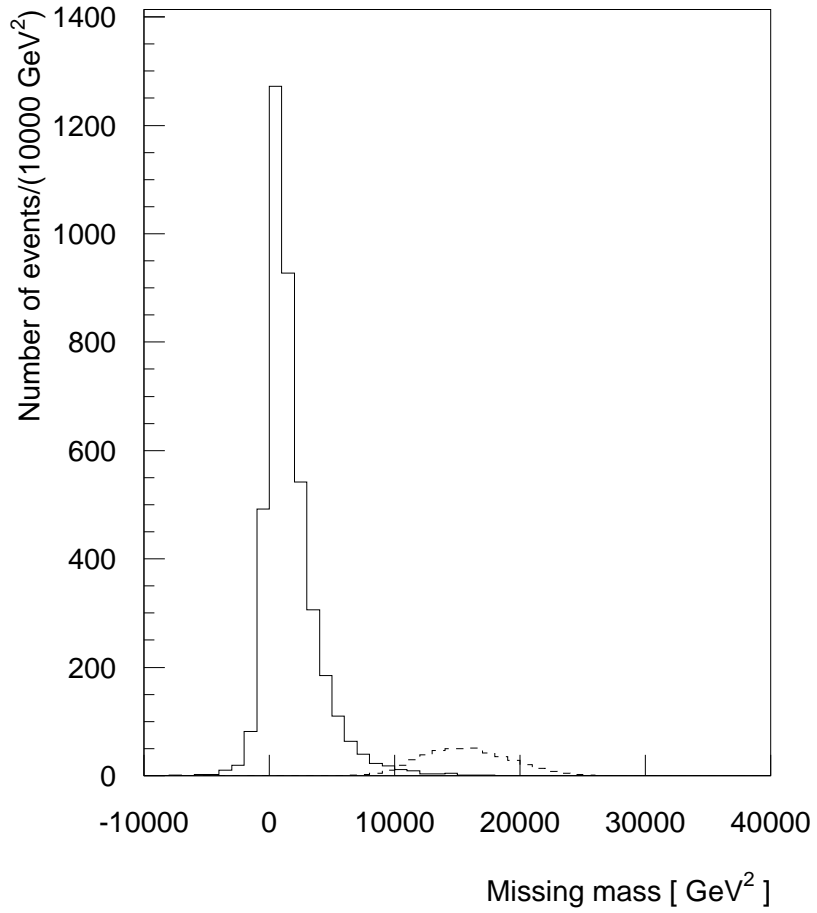


Figure 7: The missing mass distribution for the $lepton + 2jets + \cancel{E}_T$ signature for the background (solid line) and for the chargino pair production (dashed line).

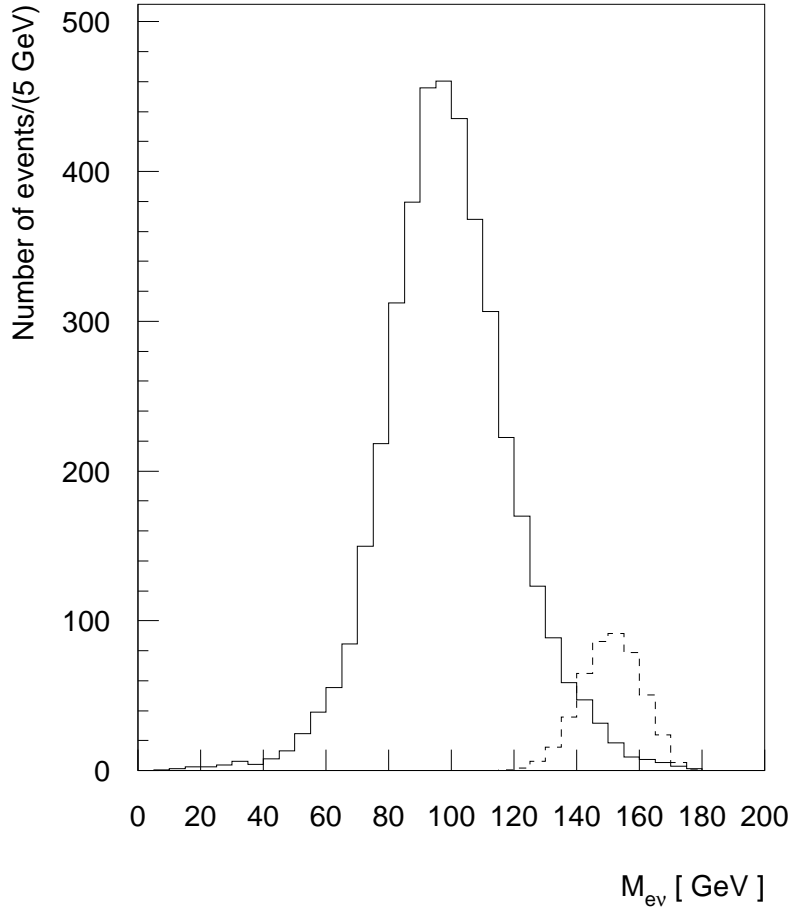


Figure 8: The invariant electron-neutrino mass distribution for the $lepton + 2jets + \cancel{E}_T$ signature for the background (solid line) and for the chargino pair production (dashed line).

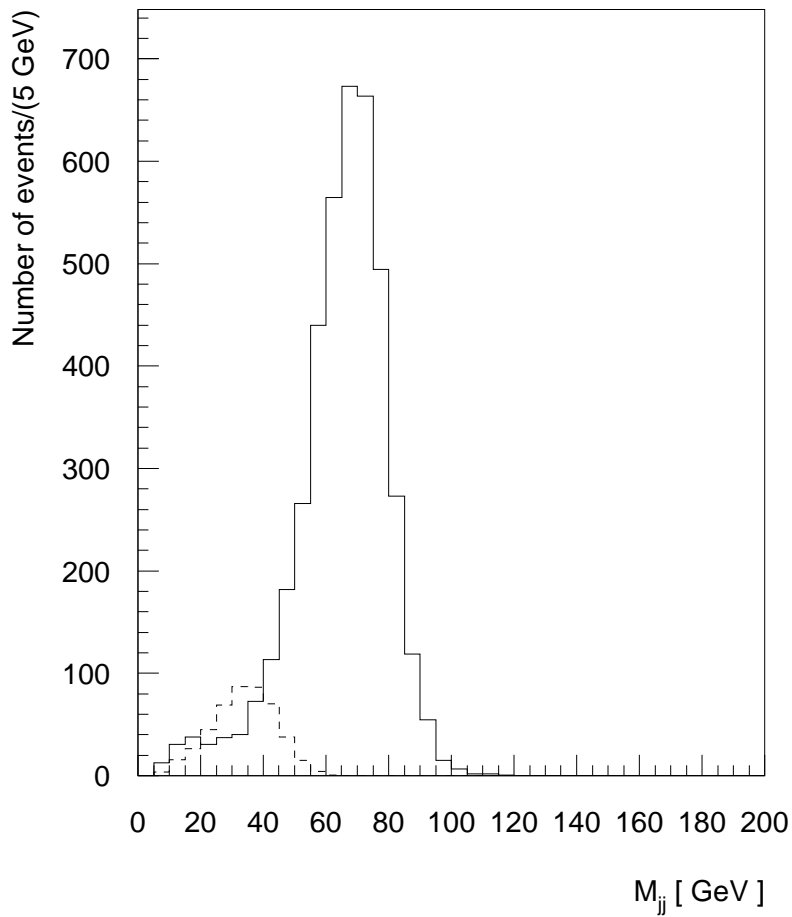


Figure 9: The di-jet mass distribution for the $lepton + 2jets + \cancel{E}_T$ signature for the background (solid line) and for the chargino pair production (dashed line).

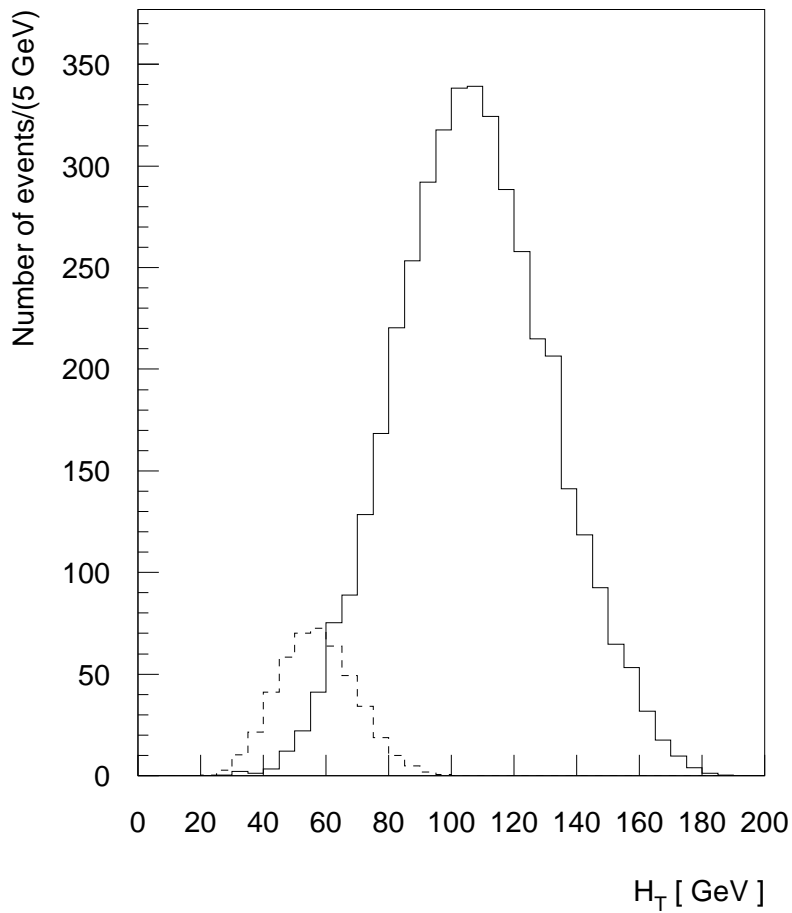


Figure 10: The H_T distribution for the $lepton + 2jets + \cancel{E}_T$ signature for the background (solid line) and for the chargino pair production (dashed line).

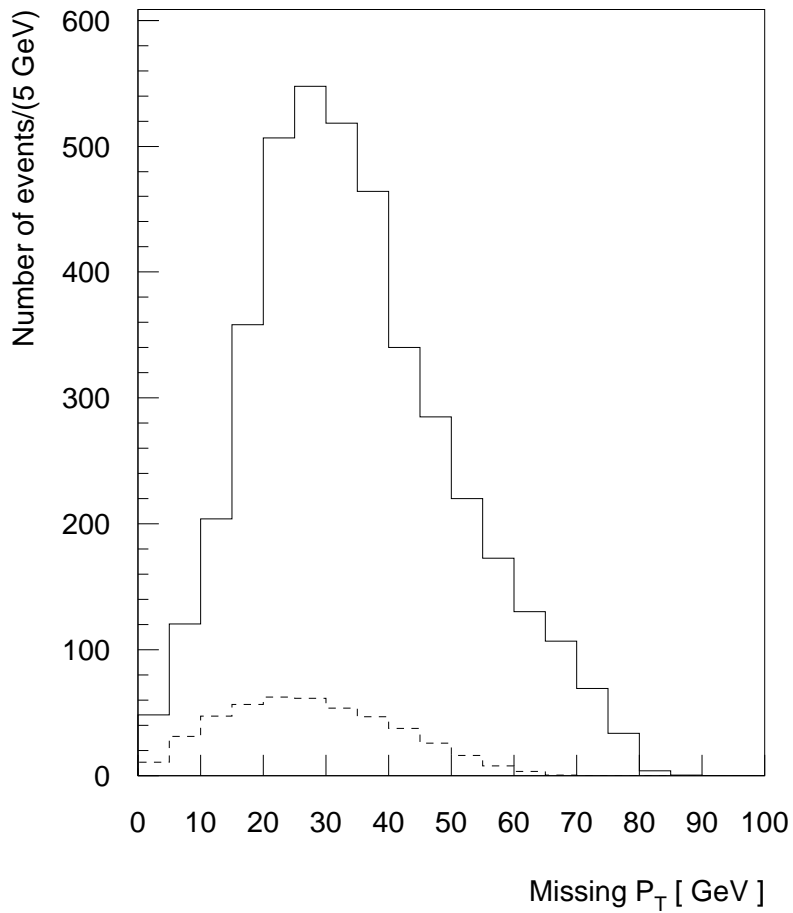


Figure 11: The \cancel{E}_T distribution for the $lepton + 2jets + \cancel{E}_T$ signature for the background (solid line) and for the chargino pair production (dashed line).

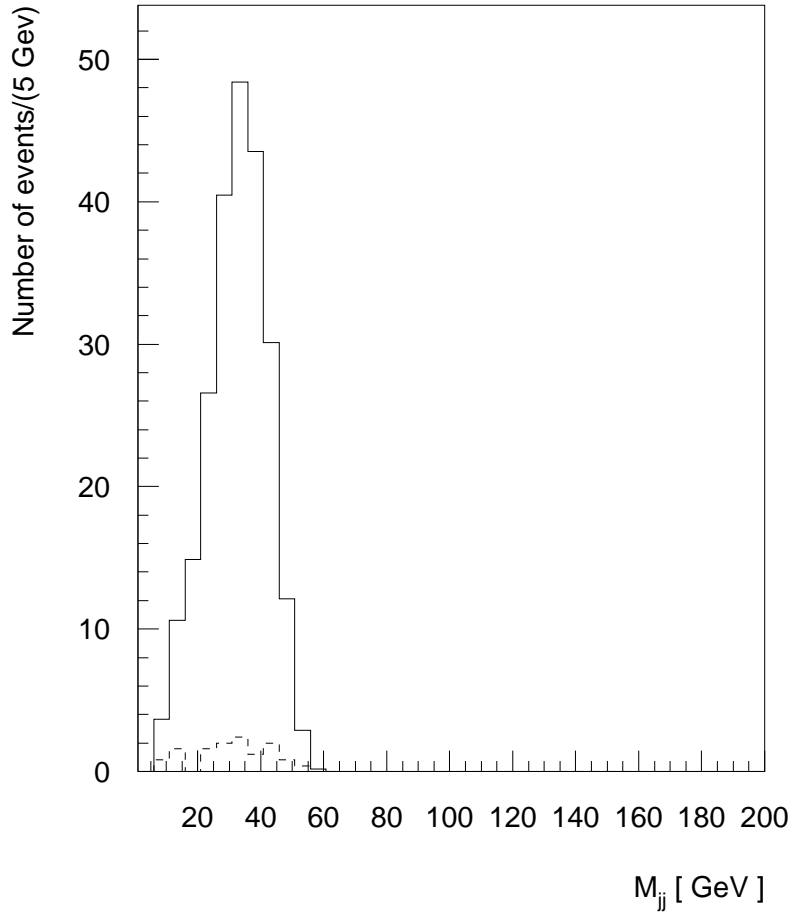


Figure 12: The di-jet mass distribution for the $lepton + 2jets + \cancel{E}_T$ signature for the signal+background (solid line) and for the background (dashed line) after cuts have been applied.

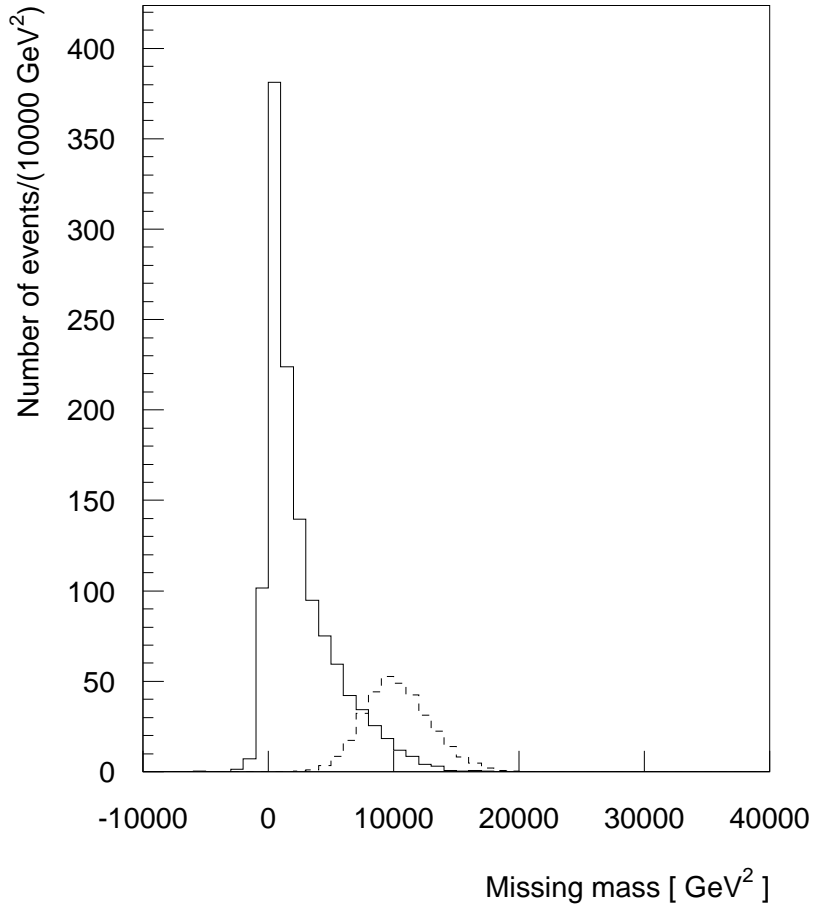


Figure 13: The missing mass distribution for the $4jets + \cancel{E}_T$ signature for the background (solid line) and for the chargino pair production (dashed line).

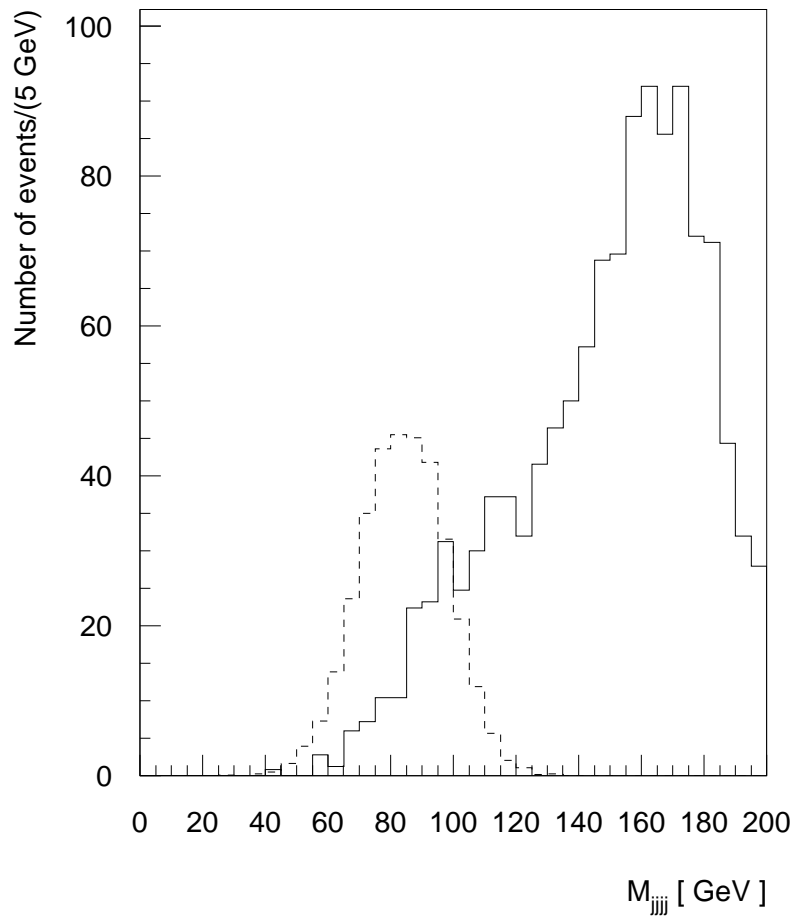


Figure 14: The di-jet mass distribution for the $4jets + \cancel{E}_T$ signature for the background (solid line) and for the chargino pair production (dashed line).

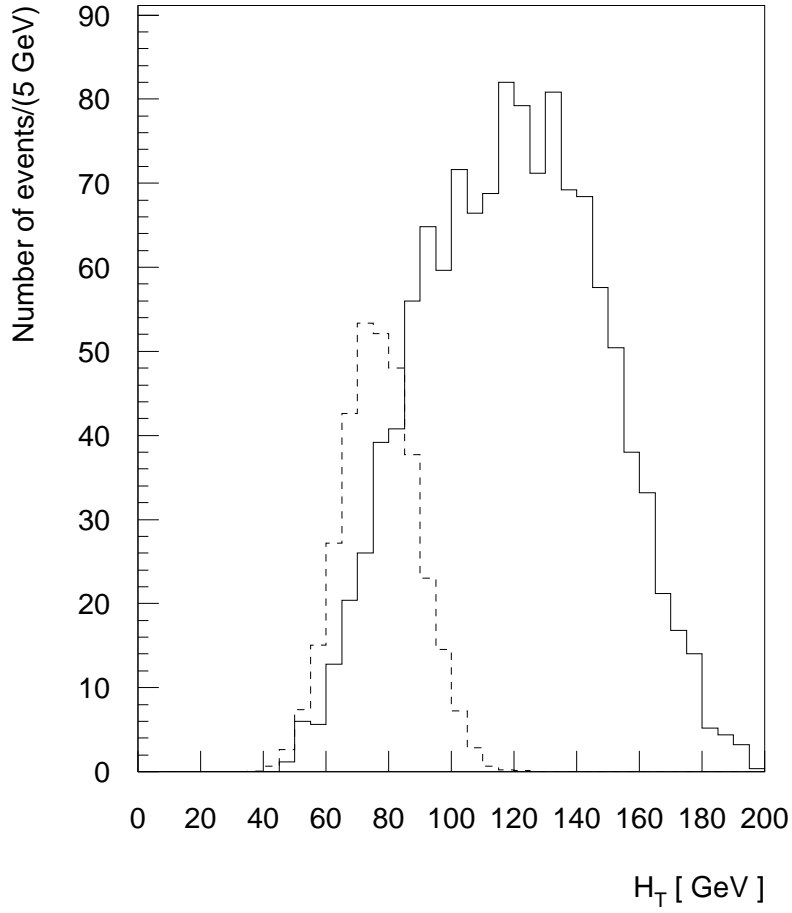


Figure 15: The H_T distribution for the $4jets + \cancel{E}_T$ signature for the background (solid line) and for the chargino pair production (dashed line).

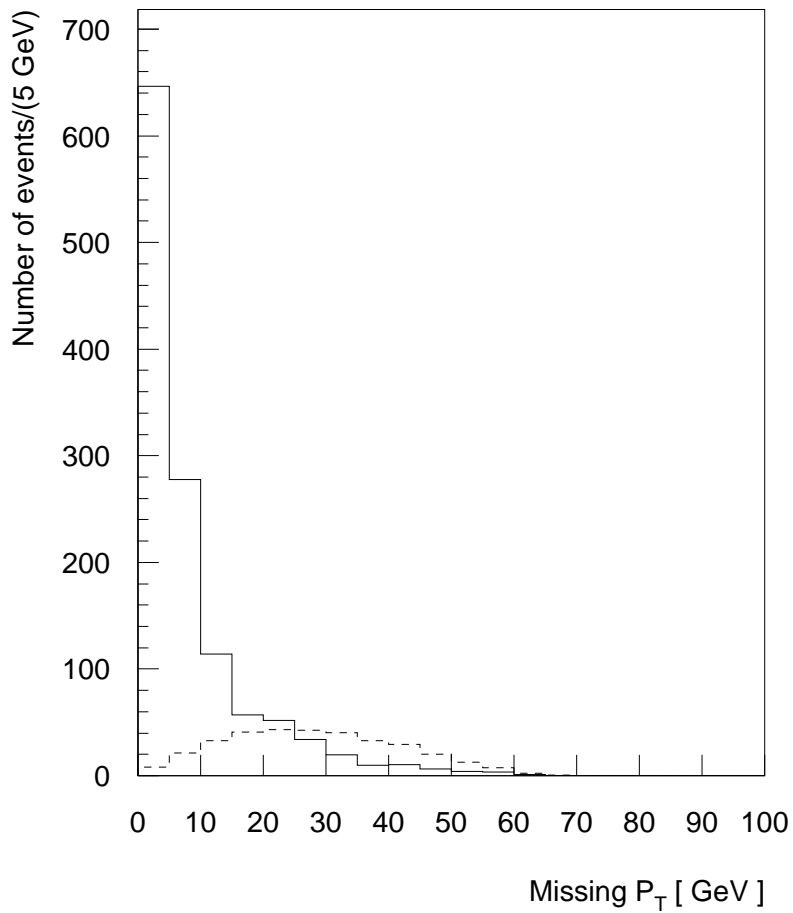


Figure 16: The \cancel{E}_T distribution for the $4jets + \cancel{E}_T$ signature for the background (solid line) and for the chargino pair production (dashed line).

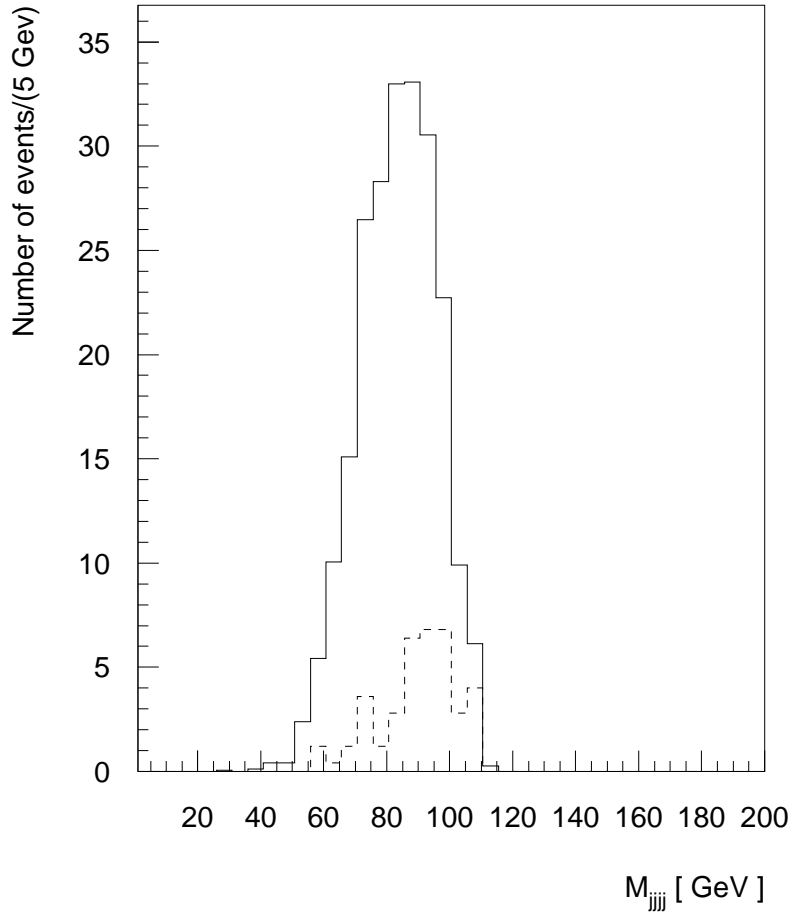


Figure 17: The di-jet mass distribution for the $4jets + \cancel{E}_T$ signature for the signal+background (solid line) and for the background (dashed line) after cuts have been applied.

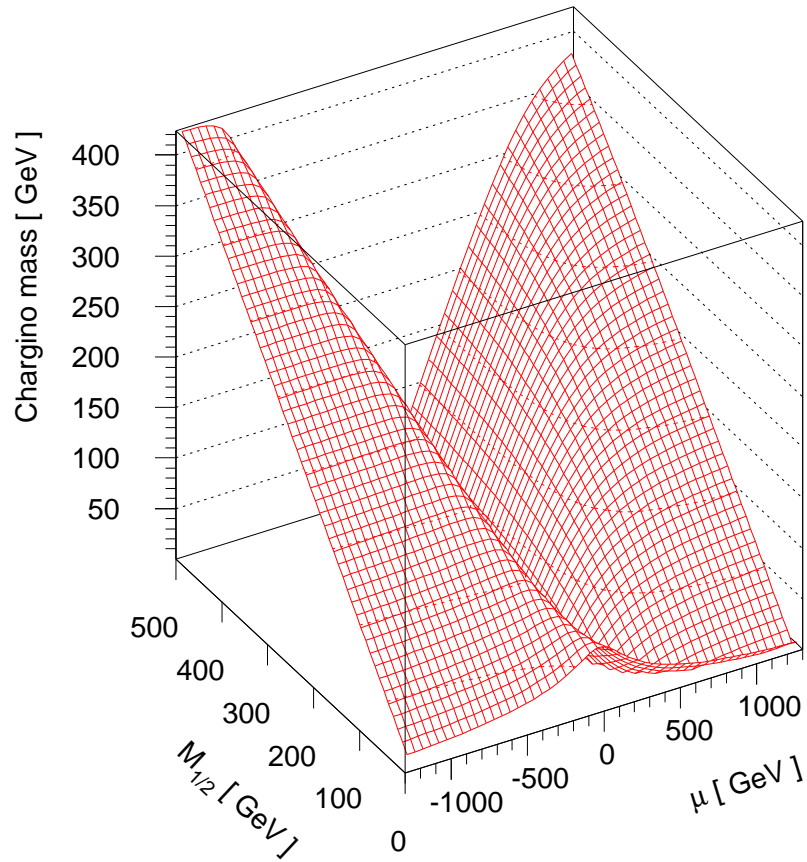


Figure 18: The chargino mass as a function of $m_{1/2}$ and μ for low $\tan\beta$

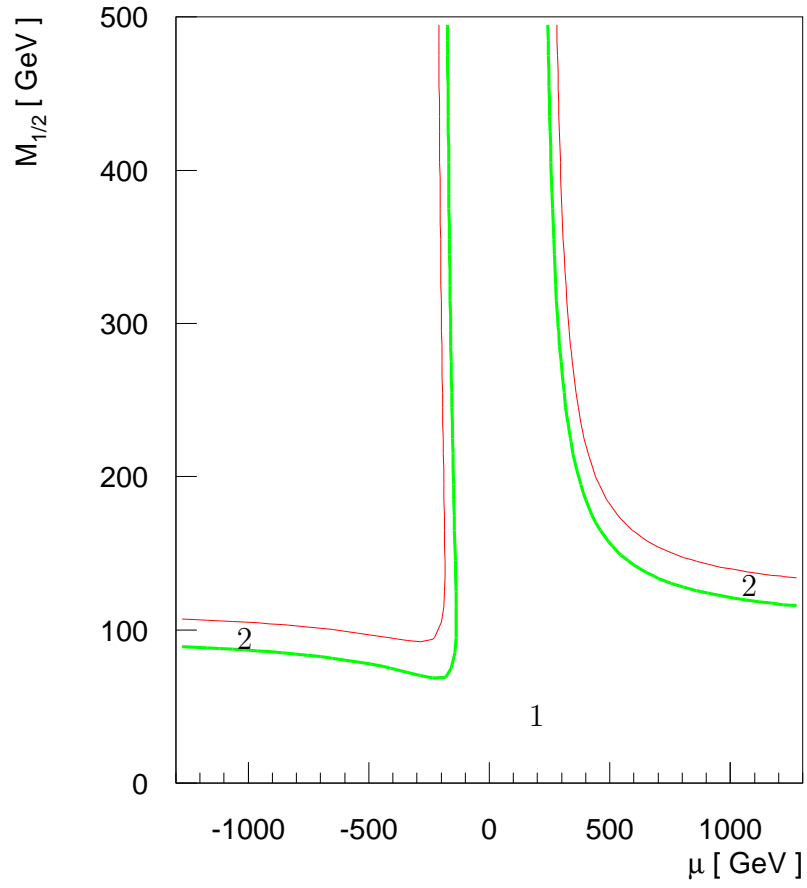


Figure 19: The region in the $m_{1/2} - \mu$ plane for low $\tan\beta$ excluded for $m_{\chi^\pm} > 85$ GeV (1) and can be excluded for LEP II $m_{\chi^\pm} > 99$ GeV (2).

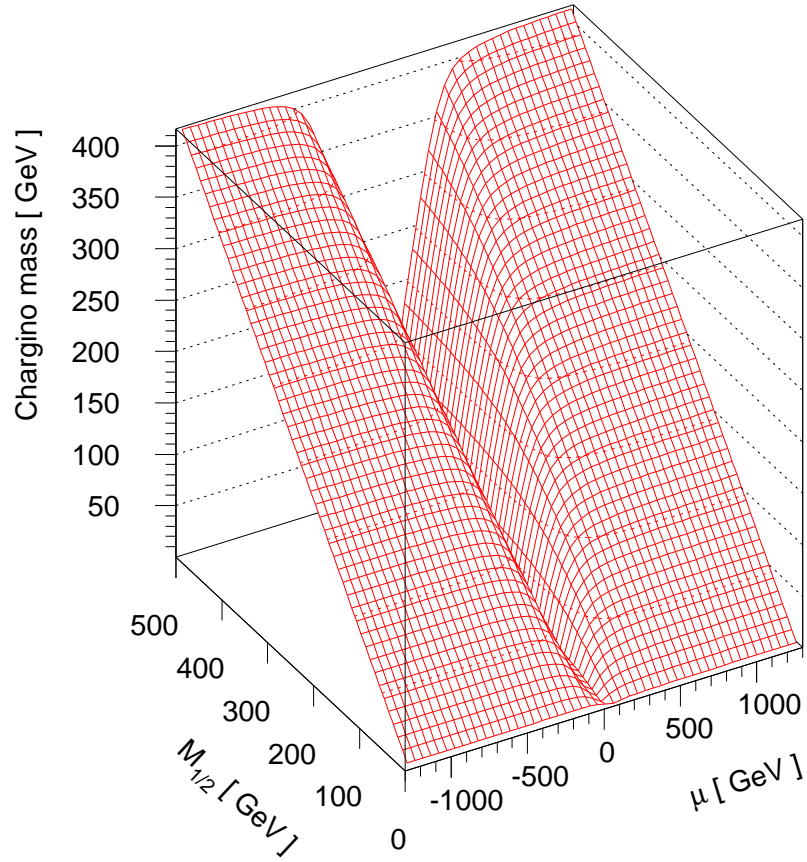


Figure 20: The chargino mass as a function of $m_{1/2}$ and μ for the high $\tan\beta$ scenario.

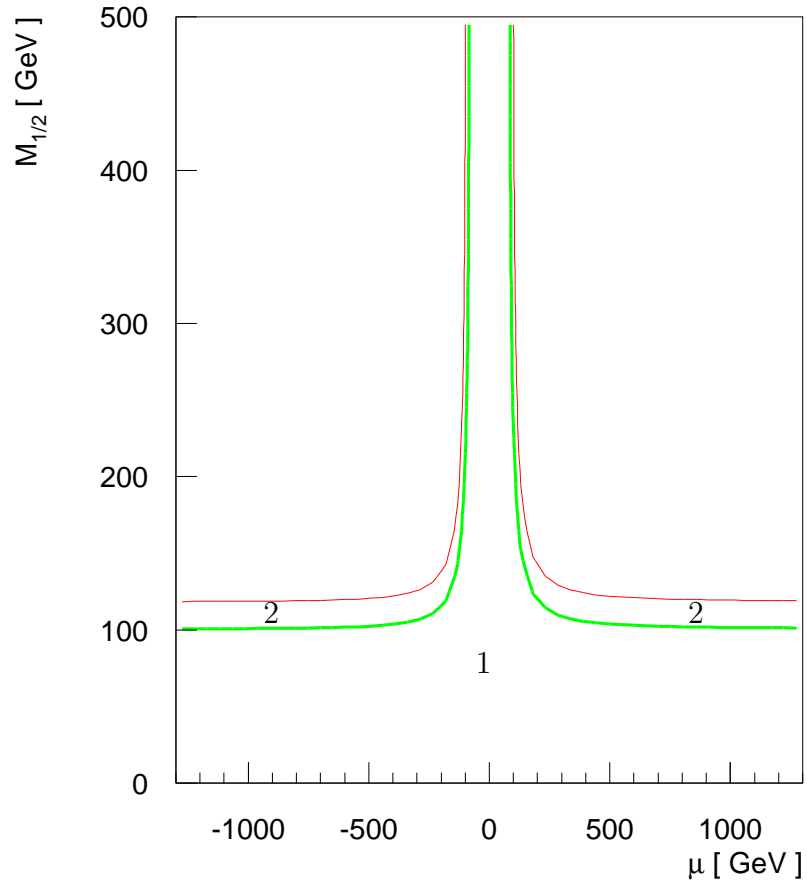


Figure 21: The region in the $m_{1/2} - \mu$ plane for high $\tan\beta$ excluded for $m_{\chi^\pm} > 85$ GeV (1) and can be excluded for LEP II $m_{\chi^\pm} > 99$ GeV (2).

Tables

| | $\tan \beta = 1.52$ | $\tan \beta = 41.2$ |
|-----------|---------------------|---------------------|
| m_0 | 400 GeV | 800 GeV |
| $m_{1/2}$ | 111 GeV | 88 GeV |
| $\mu(0)$ | 1260 GeV | -270 GeV |
| $A(0)$ | 0 GeV | 1256 GeV |

Table 1: The "best fit" SUSY parameters for the low and high $\tan \beta$ scenarios.

| | $\tan \beta = 1.52$ | $\tan \beta = 41.2$ |
|------------------------|---------------------|---------------------|
| $\tilde{\chi}_1^\pm$ | 82 GeV | 70 GeV |
| $\tilde{\chi}_2^\pm$ | 549 GeV | 304 GeV |
| $\tilde{\chi}_1^0$ | 41 GeV | 35 GeV |
| $\tilde{\chi}_2^0$ | 83 GeV | 69 GeV |
| $\tilde{\chi}_{3,4}^0$ | ≈ 540 GeV | ≈ 295 GeV |
| \tilde{t}_1 | 140 GeV | 504 GeV |
| \tilde{b}_1 | 383 GeV | 675 GeV |
| $\tilde{\nu}_\tau$ | 407 GeV | 818 GeV |

Table 2: The mass spectrum of some SUSY particles for the "best fit" for the low and high $\tan \beta$ scenarios.

| | <i>Process</i> | $\Gamma(\text{GeV})$ | <i>BR</i> (%) |
|---|---|-------------------------|---------------|
| 1 | $\chi^+ \rightarrow cb\chi^0$ | $0.83921 \cdot 10^{-7}$ | 0.0% |
| 2 | $\chi^+ \rightarrow ub\chi^0$ | $0.69445 \cdot 10^{-9}$ | 0.0% |
| 3 | $\chi^+ \rightarrow c\bar{s}\chi^0$ | $0.45610 \cdot 10^{-4}$ | 31.3% |
| 4 | $\chi^+ \rightarrow u\bar{s}\chi^0$ | $0.23505 \cdot 10^{-5}$ | 1.6% |
| 5 | $\chi^+ \rightarrow cd\chi^0$ | $0.23345 \cdot 10^{-5}$ | 1.6% |
| 6 | $\chi^+ \rightarrow ud\chi^0$ | $0.45991 \cdot 10^{-4}$ | 31.3% |
| 7 | $\chi^+ \rightarrow \tau^+\nu_\tau\chi^0$ | $0.16671 \cdot 10^{-4}$ | 11.4% |
| 8 | $\chi^+ \rightarrow \mu^+\nu_\mu\chi^0$ | $0.16303 \cdot 10^{-4}$ | 11.4% |
| 9 | $\chi^+ \rightarrow e^+\nu_e\chi^0$ | $0.16303 \cdot 10^{-4}$ | 11.4% |

Table 3: Chargino decay widths and branching ratios.

| Cut | <i>WW</i> : $l + j + \cancel{E}_T$ | <i>signal</i> : $l + j + \cancel{E}_T$ |
|-----|------------------------------------|--|
| 0 | 6600 | 900 |
| 1 | 4385 | 346 |
| 2 | 4206 | 317 |
| 3 | 31 | 301 |
| 4 | 26 | 268 |
| 5 | 26 | 268 |
| 6 | 15 | 228 |

Table 4: Numbers of events for the signal and background for the $l+2jets+\cancel{E}_T$ signature for the consecutive cut application for the integrated luminosity 1000 pb^{-1} .

| Cut | <i>WW</i> : $4jet + \cancel{E}_T$ | <i>signal</i> : $4jet + \cancel{E}_T$ |
|-----|-----------------------------------|---------------------------------------|
| 0 | 2200 | 1300 |
| 1 | 1183 | 261 |
| 2 | 176 | 212 |
| 3 | 44 | 190 |
| 4 | 44 | 190 |
| 5 | 43 | 187 |

Table 5: Number of events for the signal and background for the $4jets + \cancel{E}_T$ signature for the consecutive cut application for the integrated luminosity 1000 pb^{-1} .